**GSA DATA REPOSITORY 2015331**

***Gradients in stream power control lateral and downstream sediment flux in floods***

John D. Gartner[1]†, William B. Dade[1], Carl E. Renshaw[1], Francis J. Magilligan[2] & Eirik M. Buraas[1]

[1]Department of Earth Science, Dartmouth College, Hanover, New Hampshire, 03755, USA.
[2]Department of Geography, Dartmouth College, Hanover, New Hampshire, 03755, USA.
†Present address: Department of Geosciences, University of Massachusetts, Amherst, Massachusetts 01003, USA.

## Supplementary Methods and Results

**The Vermont and Colorado floods.** The 2011 Vermont and 2013 Colorado floods were among the largest on record in these regions, each causing over $US 1 billion in damages. In Vermont, Tropical Storm Irene dropped up to 280 mm of rain during an 8 h period on 28 Aug 2011. Many gaging stations recorded the flood of record, with recurrence intervals exceeding the 1-in-100 year flood (Magilligan et al., 2015). In Colorado, a slow moving cyclonic system produced 200 to 450 mm of rain in the Front Range from 9-16 September 2013, including the 1-in-1,000 year 24-hour rain event occurring 11-12 September in a zone from Boulder to Estes Park (Gochis et al., 2014). Both the Vermont and Colorado floods caused spatially variable erosion in the form of landslides, debris flows, bank failures, and channel incision, and equally widespread but variable deposition in the form of overbank and floodplain accumulation of fresh sediment (Anderson et al., 2015; Buraas et al., 2014; Coe et al., 2008; Magilligan et al., 2015; Yellen et al., 2014).

**Additional site characteristics:** Table DR1 shows additional characteristics of the study sites. Average precipitation is for the mouth of each basin. For the Vermont sites, mean annual discharge and $Q_{ref}$ are computed from USGS gages 1154000 on the Saxtons River and 1144000 located on the West Branch of the White River. $Q_{ref}$ is the reference discharge used in computations of $\Omega$. For the Colorado sites, mean annual discharge is not readily available because the Front Range lacks long-term streamflow records where discharge primarily reflects prevailing meteorological conditions (all long-term USGS gaging stations in the region have artificial diversions, storage, or other activities in or near the stream channel that affect the natural flow of the watercourse). $Q_{ref}$ for the Colorado sites is based on the peak flood flow at USGS gage 6727500 on Fourmile Creek, a nearby (< 6 km away) creek with a little human influence, similar to the study sites (Fourmile Creek is a different watershed than Fourmile Canyon Creek, although the watersheds have adjacent headwater drainage areas). Regional long-term denudation rates are based on Long Island Sound sediment accumulation for New England (Gordon 1979) and $^{10}$Be-derived mean erosion rates in crystalline rock in the Colorado Front Range (Dethier et al., 2014). Channel slopes are typically between 10 and 0.2 %. The upper 0.5

km of the Sanitas site are very steep, approaching 50% slopes, but the channel slope is 10% or less after 0.5 km.

**Modified Exner Equation.** The one-dimensional Exner equation for evolution of a channel bed, modified to accommodate lateral input of sediment, is given in terms of the elevation $\eta$ ($L$) above an arbitrary datum and porosity $\phi$ of the bed, specific volumetric sediment flux $q_{sx}$ ($L^2T^{-1}$) (that is average, per channel width) transported in the downstream direction $x$ in the channel water column overlying a bed with characteristic width $w$, and lateral input of sediment in the cross-stream $y$ direction from channel-adjacent banks, floodplains, and hillslopes per unit length of channel $q_{sy}$ ($L^2T^{-1}$)

$$\frac{\partial \eta}{\partial t} = -\frac{1}{1-\phi}\left(\frac{\partial q_{sx}}{\partial x} + \frac{q_{sy}}{w}\right). \quad (1)$$

Integrating across the channel to obtain a two-dimensional version of the Exner equation for a slowly-varying system yields

$$\frac{\partial A_s}{\partial t} = -\frac{1}{1-\phi}\left(\frac{\partial Q_{sx}}{\partial x} + q_{sy}\right), \quad (2)$$

where $Q_{sx}$ is the three-dimensional streamwise flux of sediment ($L^3T^{-1}$), and $A_s$ is the area of sediment mantling the bed within a channel cross section given by

$$A_s = -\int_w \eta dw', \quad (3)$$

and as depicted in Supplementary Fig. DR1.

More detailed derivations and treatments of the fundamental Exner equation can be found in, for example, Leliavsky (1955), Paola and Voller (2005), and Siviglia and Toffolon (2008).

With rearrangement of eq. 2, one obtains

$$\frac{\partial Q_{sx}}{\partial x} = q_{sy} - \varepsilon \frac{\partial A_s}{\partial t}, \quad (4)$$

where $\varepsilon \equiv 1\text{-}\phi$.

In this preliminary analysis, volumetric streamwise sediment flux $Q_{sx}$ is proposed to be linearly proportional to total stream power per channel length, which in turn is conventionally evaluated as the product of volumetric water discharge $Q$ ($L^3T^{-1}$) and channel slope $S$ in the streamwise direction. That is, $Q_{sx} \propto QS$, and thus, eq. 4 is approximated

$$\frac{\partial QS}{\partial x} \propto q_{sy} - \varepsilon \frac{\partial A_s}{\partial t}. \quad (5)$$

The key assumptions underlying the relevance and applicability of eq. 5 include channel dynamics that are limited by sediment transport (as opposed to limited by sediment supply) and that a threshold for the transport of loose sediment mantling the bed is exceeded by the flow. A dimensionless coefficient of proportionality required to render eq. 5 as an equality would include, for example, the effects of the grain size of individual particles mantling the bed as a measure of bed mobility.

Stream power $QS$ for a formative flow is a geomorphic quantity that is relatively straightforward to evaluate. With the assumptions mentioned above in mind, this quantity thus holds significant potential as a diagnostic indicator of i) channel vulnerability to erosion and/or deposition during formative discharge events and ii) the magnitude and direction of the exchange of sediment between channel and adjacent banks, floodplains and hillslopes. For example, eq. 5 implies that a positive streamwise gradient in total stream power is associated with a channel reach subject to lateral sediment input ($q_{sy}$) and/or channel incision (including channel deepening and/or widening reflected in the quantity $-\partial A_s / \partial t$). Conversely, a negative gradient in total stream power may indicate deposition of sediment in channel-adjacent settings and/or channel aggradation (including channel shallowing and/or narrowing).

**Total Stream Power.** Total stream power was estimated along the 4 rivers by DEM analysis at the time of peak flow in the 2013 Colorado Floods and 2011 Vermont Floods. We focus on total stream power because we are interested in $Q_{sx}$ for the entire flow width. This departs from several other sediment transport studies that focus on unit stream power ($\Omega/w$) because it is a close analog of shear stress (Petit et al., 2005). The following four watersheds were chosen because they were accessible and displayed abundant near-channel mass wasting and deposition: the Saxtons River (190 km$^2$) and West Branch of the White River (112 km$^2$) in Vermont, and Fourmile Canyon Creek (20 km$^2$) and an unnamed creek on Mt. Sanitas (0.8 km$^2$) in Boulder, CO. Note that Fourmile Canyon Creek differs from Fourmile Creek, which is also in Boulder County, CO and a well-studied site of the Boulder Creek Critical Zone Observatory.

DEMs were hydrologically corrected by filling spurious depressions, and flow accumulation areas were computed for each cell along river channels following methods used by the USGS StreamStats program (Ries et al., 2008). Reach slope ($S$) was computed at each cell along the stream centerline with a 200 to 1,000-m smoothing centered at the cell. This smoothing distance was based on the basin size of the study area, approximately 1/10 the square root drainage area. Discharge was estimated at each cell by the formula $Q_i = Q_{ref}\,(A_i/A_{ref})$, where $Q_i$ is discharge at the cell $i$, $Q_{ref}$ is discharge at a reference cell on the same river, $A_i$ is contributing area at cell $i$, and $A_{ref}$ is contributing area at the reference cell. For the Vermont rivers, the reference discharge was the measured peak storm discharge at nearby USGS stream gages #01154000 for the

Saxtons River and #01144000 for the White River. For the Colorado creeks, the reference discharge was the 100-year recurrence interval peak flow estimated by regression equations in the USGS StreamStats program (Ries et al., 2008) at the watershed outlet, because stream gages are not located on these creeks. This is likely a low estimate of the actual flow, given that the precipitation recurrence interval was ~1/1000 year event (Gochis et al., 2014). Stream power was computed at each cell along the midpoint of the channel. To exhibit broader downstream trends, total stream power was also smoothed over a distance of 200 to 1000 m upstream of each cell, a distance also based on the basin size of the study area. The shaded zones of increases in and decreases in total stream power were determined by the sign (positive or negative) of the first derivative of total stream power with respect to distance downstream ($d\Omega/dx$).

In this methodology, the aim is to characterize the downstream changes in stream power throughout the watershed via readily available data. As such, the actual stream power at any given location may have been quite different at the time of the peak flow due to flow routing and other measurement uncertainties. Nevertheless this analysis provides an accessible index of conditions throughout the watershed especially in comparisons between nearby reaches.

Other studies have also incorporated grain size in stream power computations (Yang, 1972), but we do not. For suspended sediment, we make the assumption that grain size of suspended sediment in transport does not vary dramatically from one reach to the next. This fits with our focus on local gradients in $Q_{sx}$ rather than thresholds and absolute magnitudes of $Q_{sx}$.

For bedload, grain size may be unimportant, based on an analysis using the Meyer-Peter and Müller (Meyer-Peter and Müller, 1948) sediment transport law and a constant friction coefficient for closure, as follows. The Meyer-Peter and Müller equation is

$$\frac{q_s}{(gRd^3)^{\frac{1}{2}}} \propto 8(\tau^* - \tau_c^*)^{\frac{3}{2}} \quad \text{(S1)}$$

where $q_s$ is total sediment discharge $Q_s$ divided by channel width $w$, $g$ is gravity, $R$ is relative excess density $(\rho_s\text{-}\rho)/\rho$, where $\rho_s$ and $\rho$ are the densities of the particles and fluid, respectively. The parameter $d$ is characteristic grain size, and $\tau^*$ and $\tau^*_c$ are the dimensionless shear stress and critical shear stress for initiation of particle transport.

Dropping the constants, including $R$ and $\tau^*_c$, the equation can be expressed as proportionality:

$$\frac{q_s}{(gd^3)^{\frac{1}{2}}} \propto \left(\frac{Sh}{d}\right)^{\frac{3}{2}} \quad \text{(S2)}$$

where $S$ and $h$ are the characteristic slope and water depth. Upon rearrangement:

$$q_s \propto (gS^3h^3)^{\frac{1}{2}} \quad \text{(S3)}$$

Here we look to replace depth $h$ with discharge (Dade et al., 2011) using the depth averaged flow speed $u$ in a quadratic drag law with friction coefficient $f$:

$$\rho g h S = \rho f u^2 \tag{S4}$$

Conservation of water mass dictates that discharge $Q \equiv uhw$, and upon rearrangement of eq. (S4) we obtain an expression for channel depth h as a function of discharge Q:

$$h = \left(\frac{f Q^2}{g S w^2}\right)^{\frac{1}{3}} \tag{S5}$$

Substituting eq. (S5) into eq. (S3), canceling repeated terms, and dropping $f$ under the assumption that it is approximately constant through the study reaches, we obtain:

$$q_s \propto \left(\frac{S^2 Q^2}{w^2}\right)^{\frac{1}{2}} \tag{S6}$$

Recalling that $q_s = Q_s/w$ and reducing, we obtain

$$Q_s \propto S\,Q \tag{S7}$$

This shows that total bedload sediment discharge $Q_s$ can be independent of bed grain size. The analysis hinges in part on the exponent (3/2) in the Meyer-peter Müller equation, eq. (S1), and more broadly on the assertion that eq. (S1) captures the important dynamics of bedload transport during floods. However, eq. (S1) is a time-tested relationship for bedload transport.

Although we examine outcomes of single, extreme events, this approach may also be applicable to longer timescales and less dramatic floods. Patterns of increases and decreases in $\Omega$ would be similar if discharge is reduced uniformly along these rivers, as expected in moderate events. The Vermont and Colorado floods caused minor, if any, changes in the locations of increases and decreases in $\Omega$. Thus, general locations of sediment sources and sinks may have persisted over longer timescales, perhaps since the last glaciation in Vermont or passage of a knickzone in Colorado (Anderson et al., 2015)

**Lateral and vertical erosion and deposition.** Near-channel erosion and deposition were quantified along 52 river km by field surveys and pre/post satellite imagery. Pre- and post-flood satellite images from Google Earth and the National Agricultural Imagery Program (NAIP) were used initially to map the locations and aerial extents of fresh sedimentary deposits on floodplains and recent mass wasting scars in the form of bank failures, landslides, landslips, and debris flows that contributed sediment to the river channel. Mass wasting consisted primarily of landslides extending up hillslopes, triggered by stream undercutting, and to a much lesser extent bank failures and debris flows. There were only a few locations were mass wasting was triggered by slope processes (e.g. excess pore pressure on steep slopes causing debris flows or gully erosion),

however we suspect that the steep slopes in many of these locations are a result, in part, of previous mass wasting events that were triggered by stream undercutting.

Aerial imagery and photographs of the flood effects are shown in Fig. DR2.

Field surveys verified the locations and extents of these features, especially in wooded areas. Typically there were clear scars at the locations of mass wasting. For erosion (including bank erosion) that was not large enough to be visible in aerial imagery, we used field evidence to estimate the volume of erosion. The average thicknesses of these features were estimated based on spot measurements, using meter tapes to estimate thickness of material removed by mass wasting relative to adjacent undisturbed topography and using shovels and probes to dig and penetrate through fresh sediment deposits to underlying leaf layers or vegetation. It was not practical to make accurate thickness measurements of each of the many and large near-bank deposits along the Vermont Rivers, thus the deposit areas are reported rather than the deposit volumes.

Erosion and deposition reflects primarily lateral inputs and outputs along the 3 larger waterways, and reflects lateral and vertical inputs and outputs along the Mt. Sanitas channel. Measurements of channel bed incision and deposition were feasible based on field evidence in the smaller watershed on Mt. Sanitas, but not practical on the 3 larger rivers given the lack of high-resolution pre-storm long profiles. Pre/post flood cross sections measured (Buraas, 2012) in 13 locations on 5 other rivers in Vermont showed bed incision $\leq$ 45 cm and bed deposition $\leq$ 15 cm. Integrated over longer reaches, these vertical exchanges may be significant, but likely not of greater magnitude than the lateral exchanges, as evidenced by near-channel deposits and landslide scars which were typically thicker than 15 to 45 cm. These cross sections help estimate possible magnitudes of in-channel deposition and incision in the 2011 Vermont flood, but they were too sparse to be useful at the resolution or extent of this study.

The inventory of erosion and deposition prioritized making approximate volumetric measurement of many features rather the highly accurate measurement of only a few features. Most of the uncertainty resides in the estimates of the thickness of these features, since the width and length of these deposits is relatively easy to measure in satellite imagery or with a meter tape. The deposit thicknesses ranged from ~10 cm to ~100 cm. Bank erosion and landslide thicknesses range from 0.5 to 5 meters. The volumes of erosion and deposition are likely within a factor of 3 of the actual value. More confidence can be placed on the *relative* volumes of landslides and erosion from one reach to the next, because biases in volumetric measurements were likely consistent through adjacent reaches.

Table DR2 shows the location, volume, and type of erosion and deposition features. Mass wasting is termed a bank failure if it does not extend beyond the top of the channel to hillslopes and terraces. Mass wasting is termed a landslide if it extends above the channel top, and we

include erosion that occurred below the channel top in the single estimate of landslide volume. Some features are unclassified.

As stated in the manuscript, a necessary condition for our model is that sediment is in transport, $Q_{sx} \neq 0$, with available sediment and thresholds for sediment transport exceeded at the location of analysis or upstream. The widespread evidence of sediment transport at our sites verifies these conditions. In addition, we made spot measurements of grain size, water depth, and channel slope to calculate shields parameter (Mueller et al., 2005). In all cases, the values were at or above the critical value of 0.05, even for large boulders.

**Non-linear effect.** Some reaches have similar rates and magnitudes of change in $\Omega$, but different magnitudes of response. As examples, Fig. 1 shows roughly equal changes from ~15-17 km, ~19-21 km, and 24-25 km, but the middle reach shows 140 $m^3$ of erosion while the up- and downstream reaches each show ~4,000 $m^3$. Similarly, Fig. 4 shows > 20,000 $m^3$ of deposition from 9.5-10.0 km, but minimal deposition and even erosion in reaches with similar declines in $\Omega$, for example from ~6.5-7.2 km and ~8-8.5 km. These discrepancies could be due to many factors, including differences in bed and bank resistance or flow hydraulics that are not captured in our stream power analysis. At ~9.5 km on Fourmile Canyon Creek, the river debouches from the canyon to a wide valley, suggesting a reduction in sediment transport competence not experienced in the upper reaches with similar declines in total stream power.

**Width.** This paper investigates changes in channel width over time due to the flooding insofar as widths were increased by mass wasting (bank erosion and landslides) at the sides of the channels, and these width changes are included in our measurements of erosion. Aerial imagery and field observations showed little to no bank narrowing in the form of in-channel deposits on the banks opposite mass wasting features or elsewhere along channels. Thus we observe that channels were prone to widening where $d\Omega/dx > 0$. In contrast, reaches were prone to overbank deposition rather than channel narrowing in locations where $d\Omega/dx < 0$ during these extreme floods. Previous work by Buraas et al. (2014) investigated changes in channel width due to erosion and deposition in the 2011 Vermont flood and found that widening occurred in locations of elevated unit stream power (>300 $W/m^2$) and elevated bend stress (>1 $m^{2/3}$). These results are based on at-a-point measurements. As discussed in the main text, our approach departs from the body of work that focuses on at-a-point magnitudes of forces by showing the additional importance of downstream gradients in sediment transport.

Regarding changes in width over distance downstream, we also investigate if downstream changes in flow width and channel width are associated with zones of erosion or deposition, which would point to factors controlling the geomorphic response that are not captured in our stream power analysis. Downstream changes in width can influence flow hydraulics during flood events and therefore exert a control on local sediment transport dynamics and the geomorphic response. For example, Miller (1995) found that “Zones of catastrophic erosion associated with

valley expansions were generally limited to a short reach extending no more than 1-3 multiples of the downstream valley width from the expansion."

Fourmile, Sanitas, and the West Branch all showed notable flow expansions and contractions, Several locations exhibited increases in flow width of up to 500% in less than 1 river km, and other locations showed equivalent decreases over similar distances (Figs DR6d, DR7d, and DR8). Flow widths were digitized primarily based on post-flood aerial imagery that showed fresh deposits and scour in fields and sparsely vegetated areas. The field surveyed extents of deposition in fields and forests provided additional information to delineate widths. Using aerial imagery is difficult in densely forested areas, and many locations do not have reliable width measurements, especially in the smaller, headwater reaches. The locations with unreliable width measurements are evident as the data gaps in these figures (in Fig DR6d from 0 to ~7 km; in Fig DR7d from 0 to ~8.5 km; and in Fig DR8d from 0 to 0.25 km, 0.95 to 1.08 km, and 1.2 to 1.45 km). For the Saxtons River, the only available immediate post-flood imagery is panchromatic and not suitable to evaluate the flood flow width even in sparsely vegetated areas. In subsequent color imagery in 2013 on the Saxtons River, flood flow widths were not evident due to farming, road repairs and other human activities. Thus we do not report flow width data for the Saxtons River.

The data suggest that changes in flood flow width are not a dominant control on the geomorphic response, and downstream gradients in $\Omega$ better predict locations of erosion and deposition. To examine the possible effect of these substantial downstream changes in flow width on the geomorphic response we examined areas of notable increases or decreases in flow width (for example, more than doubling or halving in width along a distance less than 1 km). We tabulated the response as either erosional, depositional or no response (Table DR3). In the locations where flood width widens there is a slight tendency for deposition, with 57% of locations expressing deposition. In locations where the flood flow narrowed, the number of depositional reaches roughly equaled the number of erosional reaches.

Downstream changes in channel width (equivalent to the bankful width) were more subtle than changes in flood flow width, suggesting that local deviations in width were not a dominant control on locations of erosion and deposition. During field surveys we observed locations where bankful width increased locally by a few meters at most, but we saw no evidence of downstream increases in channel width of more than 50% per km. At these rivers, it is not feasible to examine continuous changes in channel width without extensive fieldwork. Aerial image analysis is not reliable, as confirmed by Buraas et al. (2014), because the banks are typically densely vegetated. Empirical relationships between bankful width and drainage area express overall downstream trends in bankful width (Beiger, 2015), but do not capture the local deviations from this trend. Nonetheless, the available observations suggest that the downstream changes in channel width are not a dominant control on the locations of erosion and deposition in these flood events. The channel width variations were substantially less than flow width variations, and the more

dramatic flow width variations were not a dominant control on the geomorphic response compared to downstream gradients in Ω.

Empirical equations that relate bankful width to drainage area can allow predictive modeling of unit stream power, ω, which is Ω divided by width. This approach is similar to how one might predict unit stream power absent detailed hydraulic modeling, although it does not depict how local variations in width might modulate unit stream power. Here we use equations from Bieger et al. (2015). This analysis has the assumption that most of the flood flow is contained in the channel, which can be a reasonable assumption since flow velocities on floodplains are relatively low due to higher roughness compared to the channel. Modeled ω and Ω express similar patterns, largely because the width is a function only of drainage area, which increases monotonically downstream (Figs DR5c, DR6c, DR7c, and DR8c). Magilligan (1992) suggested a threshold of ω of 300 $W/m^2$, above which extreme geomorphic changes occur. At our sites, we observed a general lack of abundant near-channel erosion or deposition in the first 4 km of the Saxtons and 5 km of the West Branch, but notable erosion occurred at the start of the Sanitas channel at 0 km. In support of this threshold value, ω first exceeded 300 $W/m^2$ at ~4 km on the Saxtons and 0 km on the Sanitas channel. On the West Branch, ω first exceeded 300 $W/m^2$ at ~1.5 km which coincides with the start of bank erosion and deposition; however, large landslides and deposits did not occur until ~ 5 km where ω exceeded 1000 $W/m^2$. In each stream, ω remains above 300 $W/m^2$ in the middle and lower reaches, but the type of response—erosion or deposition—does not depend on the magnitude of ω at a single point along the river. The unit stream power data displayed in these figures reinforces a central point of this paper. Once the thresholds for sediment transport are exceeded, erosion or deposition can occur depending on whether the total sediment transport is increasing or decreasing relative to neighboring upstream locations.

**Geologic controls.** The manuscript states that geologic maps (Colton, 1978; Ratcliffe et al., 2011) suggest that slope variations are partly controlled by varying resistance of underlying bedrock and relict glacial features (consistent with Hack, 1957, 1973). However, some changes in geologic boundary conditions are too subtle to be evident at the resolution of geologic maps. We see an interplay between lithology and slope in a few locations. For example, the transition from mica schist to phyllite on the West Branch of the White occurs at 8 km (Fig. DR3b), and this coincides with a transition from decreasing to increasing channel slope (Fig. DR6b). This suggests the more resistant mica schist forms a knickpoint. There is also a sharp decrease in slope at 9 km where the river turns southeast and follows the strike of the phyllite unit (strike is not published on the geologic map, but is evident in the field and in regional patterns of folding). Mt. Sanitas shows another example of geologic controls, both evident and not evident in the geologic mapping. There is a distinct decrease in slope from 0.35 to 0.5 km (Fig DR8b) as the creek crosses from the sandstone to the shale lithology (Fig DR3c). However, within the mapped shale lithology there are additional increases and decreases in slope between 0.5 and 1.0 km due to changes in bedrock competence that are observable in the field but not indicated on the

geologic map. In sum, we observe changes in slope at changes in lithologic boundary conditions, sometimes evident in published maps and sometimes not.

A direct relationship between lithology and type of flood response is not strongly supported at these sites, based on information available in the geologic maps. Both mass wasting and deposition occur in abundance in every mapped lithology in Colorado and Vermont along these rivers. For example, along the West Branch of the White River a preponderance of deposition occurs in some locations of the phyllite unit, but this rock type also expresses numerous large landslides. We might expect the mass wasting to occur primarily where the channel follows the strike of this unit, but this pattern is not evident. Landslides occurred where the river course is on strike (southeast) and cross strike (northeast). Likewise, deposition occurs where the river is both on strike and cross strike. Stream power gradients better predict the tendencies toward erosion or deposition within this phyllite unit, as shown in the manuscript in Fig. 2b from 8 to 16 km.

In Vermont, many landslides occurred in locations of relatively thick glaciofluvial deposits. This may partly explain why there is not a strong relationship between lithology and a tendency for landslides—the distribution of material that mantles the bedrock, rather than the bedrock itself, may have a stronger influence on the distribution of landslides. Unfortunately, surficial geology maps (Fig. DR4) do not depict these variations in material (Doll, 1970). The description from the surficial geology map along large sections of the studied rivers is "Till mantling the bedrock and reflecting the topography of the underlying bedrock surface. Thicker in the valleys and thinner in the uplands. On many exposed uplands postglacial erosion has left only rubble and scattered boulders on bedrock." Other mapped surficial facies in our study areas, including kame terraces, outwash, and recent alluvium, do not exhibit a propensity for erosion or deposition.

In Colorado, Anderson et al. (2015) suggest that the long-term accumulation of colluvium in headwater channels made sites susceptible to debris flows and scour in the Colorado floods. A similar effect may exist at the margins of larger channels, where the accumulation of colluvium and soil production over long time periods may make some sites more susceptible to landslides than others. However, these subtle variations in surficial material are not depicted in geologic maps of the region, which only depict surficial deposits in broad areas to the east of these study sites (Colton, 1978; Green, 1992). Similar to the Vermont sites, surficial units did not control whether erosion or deposition occurred. Overall, improved predictions of the geomorphic response to flooding might be obtained by more detailed analysis of the bedrock and surficial geology, at a higher resolution than is commonly found in published maps, but this would require extensive field work.

**Data Repository References**

Anderson, S. W., Anderson, S. P., and Anderson, R. S., 2015, Exhumation by debris flows in the 2013 Colorado Front Range storm: Geology, v. 43, no. 5, p. 391-394.

Bieger, K., Rathjens, H., Allen, P. M., and Arnold, J. G. 2015, Development and Evaluation of Bankfull Hydraulic Geometry Relationships for the Physiographic Regions of the United States: JAWRA Journal of the American Water Resources Association, v. 51 p. 842-858, DOI: 10.1111/jawr.12282

Buraas, E. M., 2012, Assessing the geomorphic response to Tropical Storm Irene induced flooding on unregulated gravel bed rivers in New England [M.S. thesis]: Hanover, Dartmouth College, 105 p.

Buraas, E. M., Renshaw, C. E., Magilligan, F. J., and Dade, W. B., 2014, Impact of reach geometry on stream channel sensitivity to extreme floods: Earth Surface Processes and Landforms, v. 39, no. 13, p. 1778-1789.

Coe, J. A., Kinner, D. A., and Godt, J. W., 2008, Initiation conditions for debris flows generated by runoff at Chalk Cliffs, central Colorado: Geomorphology, v. 96, no. 3-4, p. 270-297.

Dade, W. B., Renshaw, C. E., and Magilligan, F. J., 2011, Sediment transport constraints on river response to regulation: Geomorphology, v. 126, no. 1-2, p. 245-251.

Dethier, D.P., Ouimet, W., Bierman, P.R., Rood, D.H., and Balco, G., 2014, Basins and bedrock: Spatial variation in $^{10}$Be erosion rates and increasing relief in the southern Rocky Mountains, USA: Geology, v. 42, p. 167–170, doi:10.1130/G34922.1.

Doll, C. G., 1970, Surficial geologic map of Vermont: Vermont Geological Survey, Department of Water Resources, scale 1:100,000.

Green, G.N., 1992, The Digital geologic map of Colorado in ARC/INFO format: U.S. Geological Survey Open-File Report 92-0507, 9 p.; http://pubs.usgs.gov/of/1992/ofr-92-0507/

Gochis, D., Schumacher, R., Friedrich, K., Doesken, N., Kelsch, M., Sun, J., Ikeda, K., Lindsey, D., Wood, A., and Dolan, B., 2014, The great Colorado flood of September 2013: Bulletin of the American Meteorological Society.

Leliavsky, S., 1955, Introduction to fluvial hydraulics: London, Constable.

Magilligan, F. J., Buraas, E., and Renshaw, C., 2015, The efficacy of stream power and flow duration on geomorphic responses to catastrophic flooding: Geomorphology, v. 228, p. 175-188.

Meyer-Peter, E., and Müller, R., 1948, Formulas for bed-load transport: Proceedings of the 2nd Meeting of the International Association for Hydraulic Structures Research, Stockholm, p. 39-64.

Nicholson, S.W., Dicken, C.L., Horton, J.D., Foose, M.P., Mueller, J.A.L., and Hon, R., 2006, Preliminary integrated geologic map databases for the United States: Connecticut, Maine, Massachusetts, New Hampshire, New Jersey, Rhode Island, and Vermont: U.S. Geological Survey Open-File Report 2006-1272.

Paola, C., and Voller, V. R., 2005, A generalized Exner equation for sediment mass balance: Journal of Geophysical Research-Earth Surface, v. 110, no. F4.

Petit, F., Gob, F., Houbrechts, G., and Assani, A., 2005, Critical specific stream power in gravel-bed rivers: Geomorphology, v. 69, no. 1, p. 92-101.

Ries, K. G., Guthrie, J. D., Rea, A. H., Steeves, P. A., and Stewart, D. W., 2008, StreamStats: a water resources web application: US Geological Survey Fact Sheet 2008-3067.

Siviglia, A., and Toffolon, M., 2008, Quasi-two-dimensional enhancement of the De Saint Venant-Exner coupled model for unsteady simulations in natural channels: *in* River, Coastal and Estuarine Morphodynamics: RCEM 2007 (eds. Dohmen-Janssen, C. M. and Hulscher, S. J. M. H.), London, Taylor & Francis.

Yang, C. T., 1972, Unit stream power and sediment transport: Journal of the Hydraulics Division, v. 98, no. 10, p. 1805-1826.
Yellen, B., Woodruff, J. D., Kratz, L. N., Mabee, S. B., Morrison, J., and Martini, A. M., 2014, Source, conveyance and fate of suspended sediments following Hurricane Irene. New England, USA: Geomorphology, v. 226, p. 124-134.

## Data Repository Figure Captions

**Figure DR1. Definition sketch for channel cross section.** $Q_{sx}$ is volumetric sediment flux transported in the downstream direction $x$; $q_{sy}$ is the magnitude of cross-stream $y$ direction volumetric input of sediment from channel-adjacent banks, floodplains and hillslopes per unit length of channel; $A_s$ is cross-sectional area of sediment mantling the bed per unit length of channel; $w$ is width of channel.

**Figure DR2. Examples of floodplain deposition and mass wasting, representing flux out of and into the channel, respectively.** A: Floodplain deposition on White River, VT. B: Floodplain deposition on Fourmile Canyon Creek, CO. C: Mass wasting on the Saxtons River, VT. D: Mass wasting on Fourmile Canyon Creek, CO. E: Aerial image of entire study reach on Mt. Sanitas, CO. F: Floodplain deposition in fields and woods on White River, VT. (Google Earth is the source for aerial imagery in panels A, B, E, and F.)

**Figure DR2. Examples of deposition and erosion, representing flux out of and into the channel, respectively.** A: White, pre-flood, 2009. B: White, post-flood, 2011. C: Sanitas, pre-flood, 2012. D: Sanitas, post-flood, 2013. E: Fourmile, pre-flood, 2012. F: Fourmile, post-flood, 2013. G: Saxtons, landslide, 2011. H: White, floodplain deposition. I: Sanitas, channel erosion, 2013. J: Sanitas, channel deposition, 2013. K: Sanitas, floodplain deposition. L: Fourmile, bank erosion, 2013. M: Fourmile, landslide, 2013. N: Fourmile, deposition, 2013.

**Figure DR3. Bedrock Geology.** Lithology at study sites with streams (white lines), deposition locations (white circles), and erosion locations (white triangles). A: Saxtons River, Vermont. B: West Branch of White River, Vermont, USA. C: Mt. Sanitas, Colorado, USA. D: Fourmile Canyon Creek, Colorado, USA (black and white dashed line shows upstream section that was not surveyed for erosion and deposition). Vermont geology from Nicholson (2006). Colorado geology from Green (1996). Shaded relief from 10 m DEM (USGS National Map).

**Figure DR4. Surficial Geology.** Surficial geology at study sites, where available, with streams (white lines). A: Saxtons River, Vermont. B: West Branch of White River, Vermont, USA. C: Fourmile Canyon and Mt. Sanitas, Colorado, USA. Vermont data from Doll (1970). Colorado data from Green (1992).

**Figure DR5. Saxtons River.** A: Long profile. B: Channel slope. C: Total stream power (blue line) and unit stream power (red line), 1 km smoothing.

**Figure DR6. West Branch of White River.** A: Long profile. B: Channel slope. C: Total stream power (blue line) and unit stream power (red line), 1 km smoothing. D. Flow width. No data for vegetated areas where flow width was unclear in aerial imagery.

**Figure DR7. Fourmile Canyon Creek.** A: Long profile. B: Channel slope. C: Total stream Power (blue line) and unit stream power (red line), 0.5 km smoothing. D. Flow width. No data for vegetated areas where flow width was unclear in aerial imagery.

**Figure DR8. Mt. Sanitas channel.** A: Long profile. B: Channel slope. C: Total stream power (blue line) and unit stream power (red line), 0.2 km smoothing. D. Flow width. No data for vegetated areas where flow width was unclear in aerial imagery.

Figure DR1. Definition sketch for channel cross section

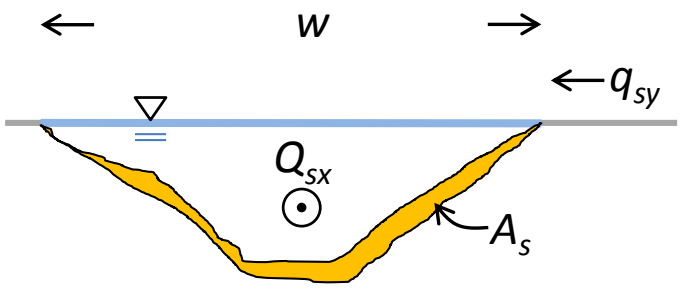

# Figure DR2. Examples of deposition and erosion

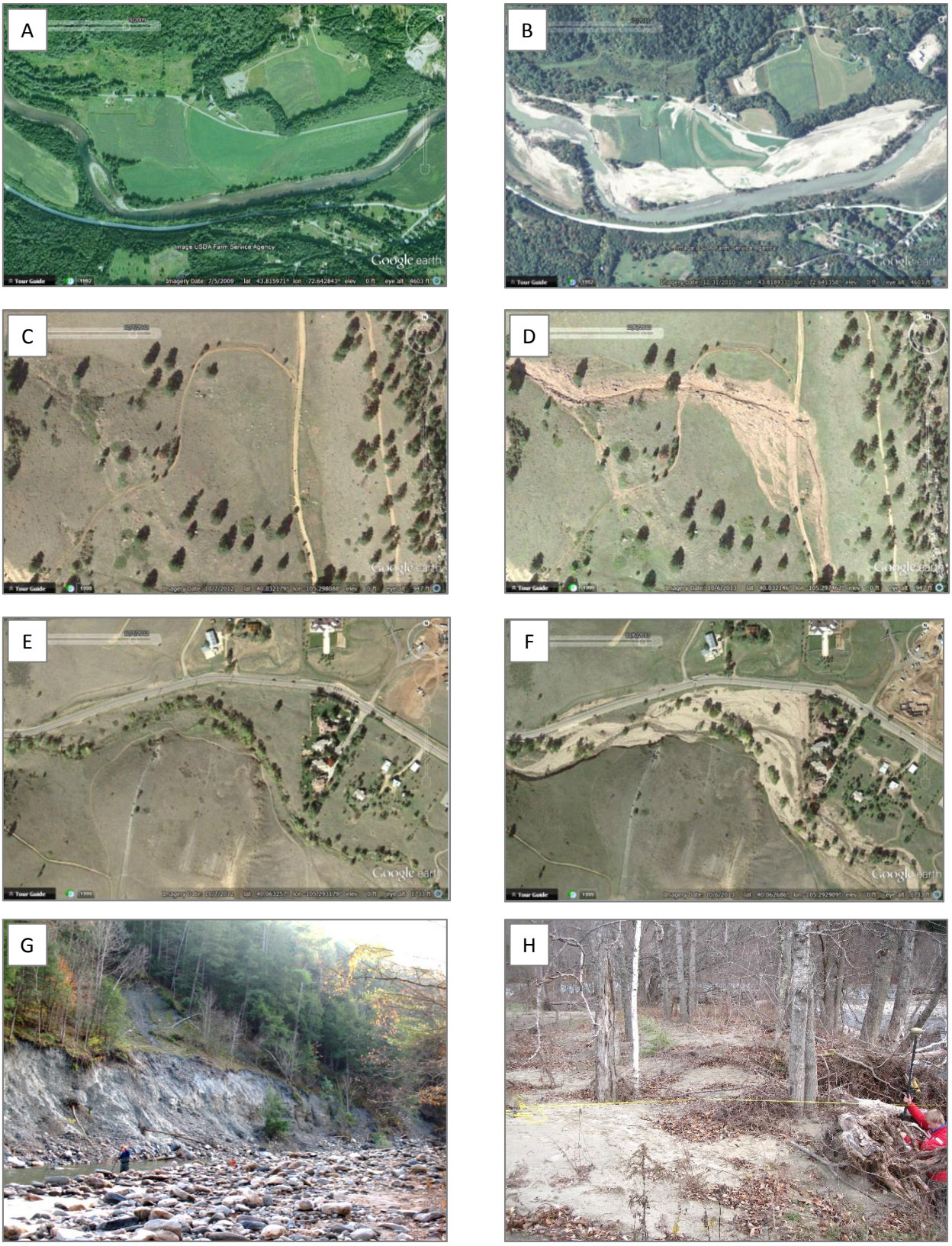

Figure DR2 (continued). Examples of deposition and erosion






Figure DR3. Lithology at study sites

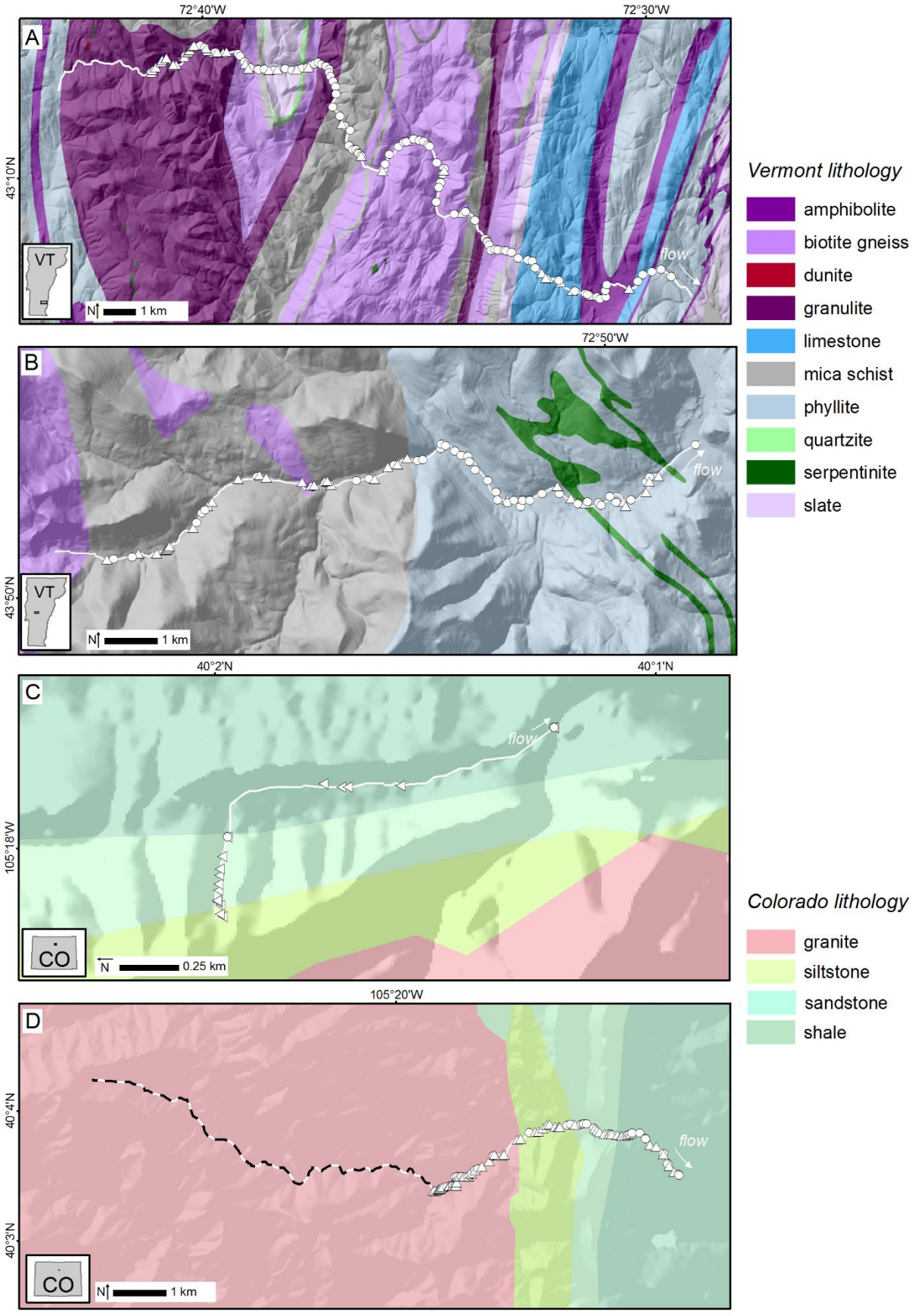

Figure DR4. Surficial geology at study sites

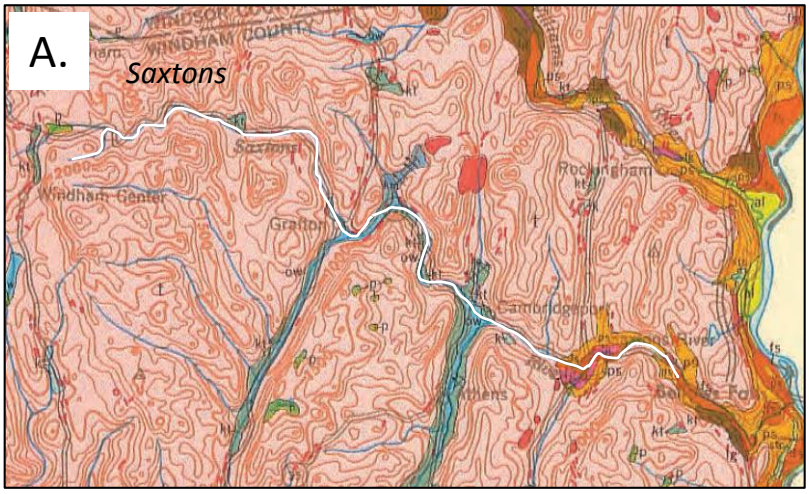


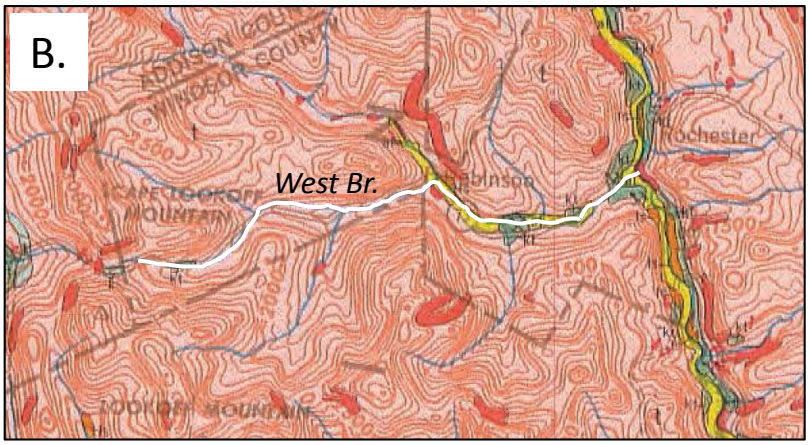


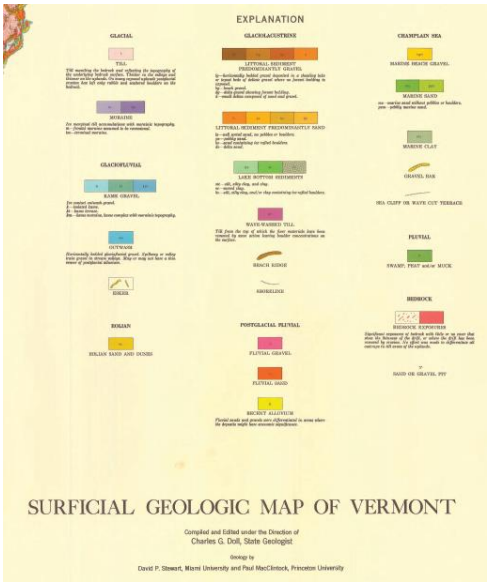


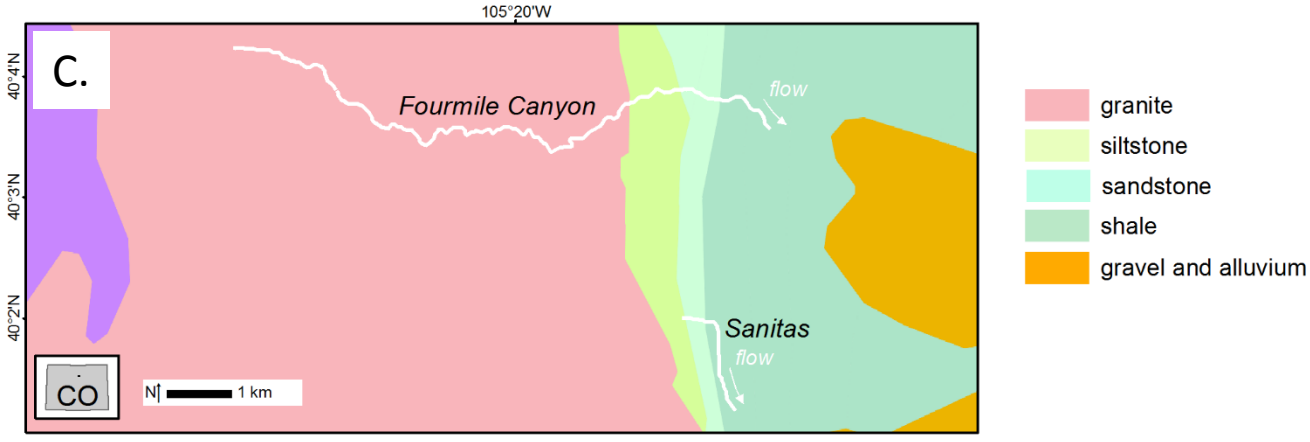

Figure DR5. Saxtons River.

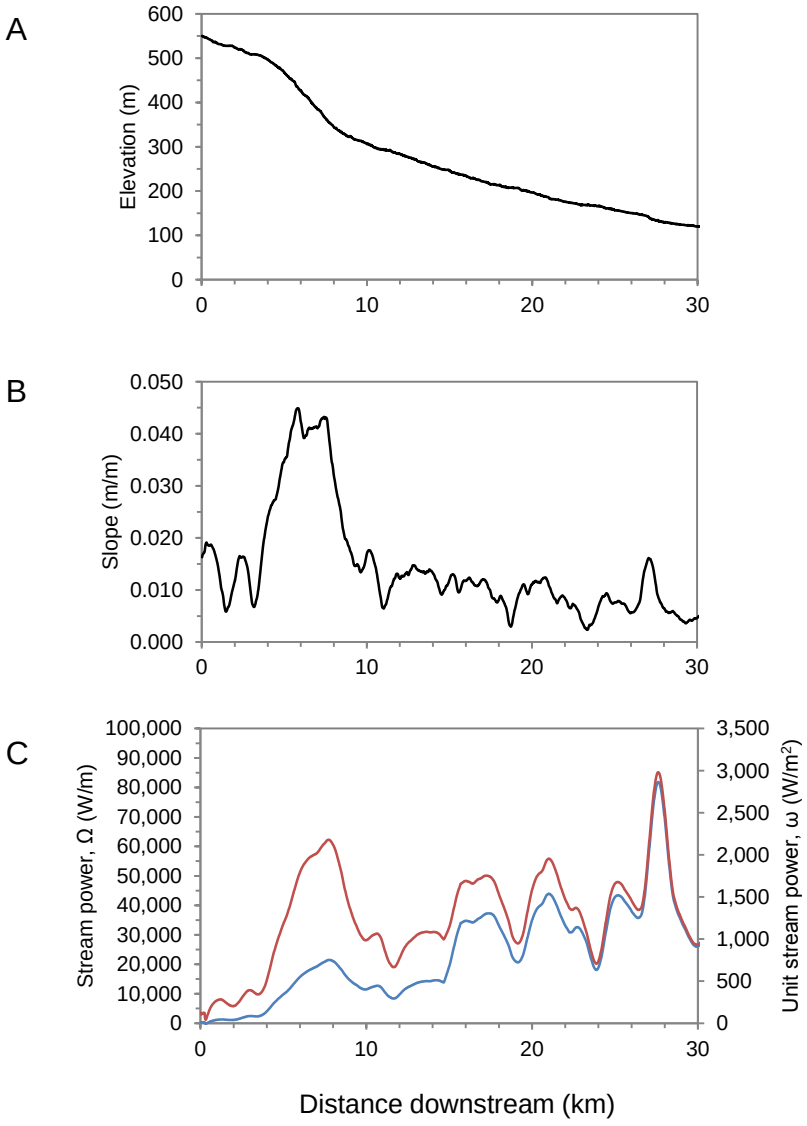

Figure DR6. West Branch of White River.

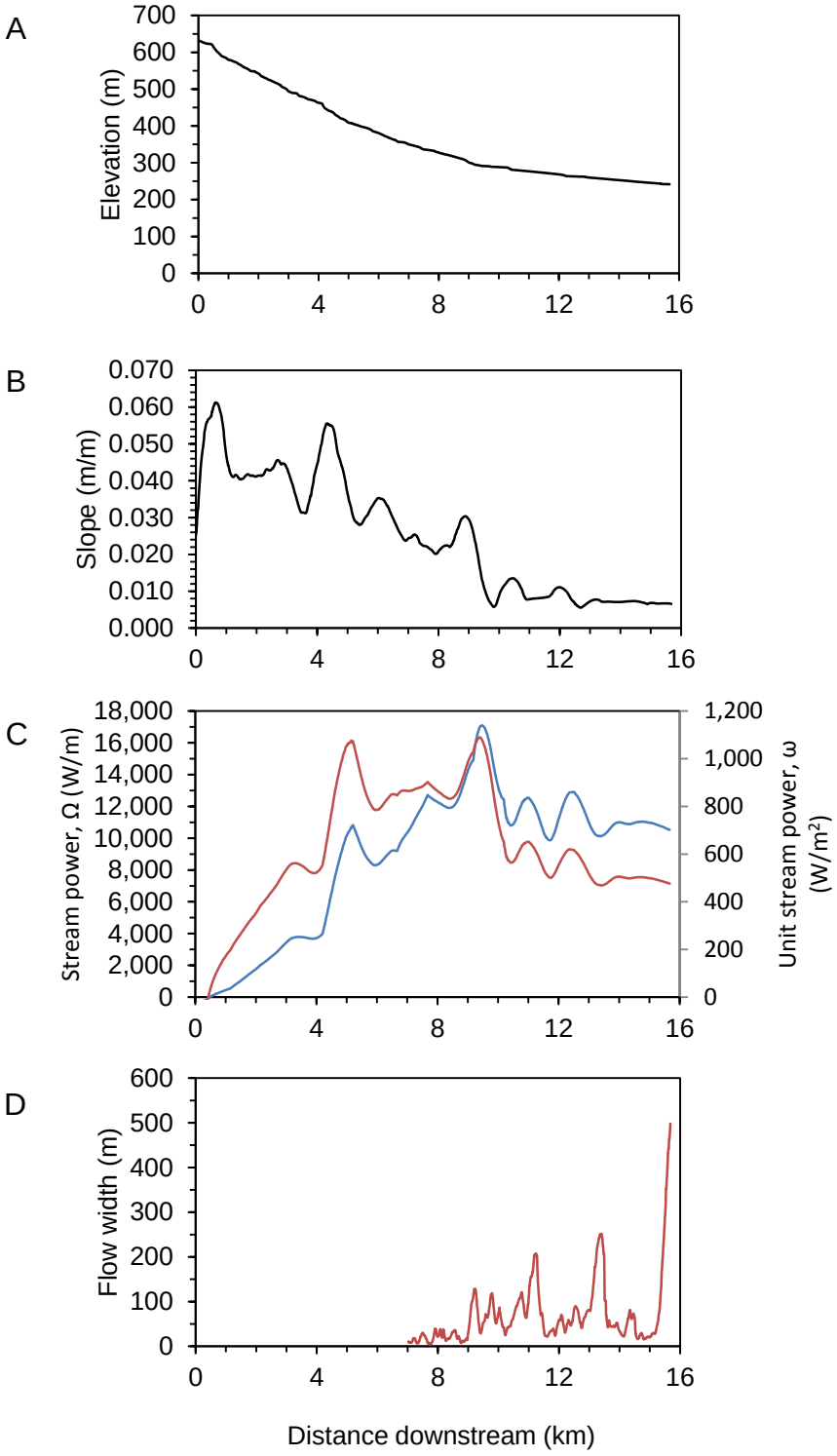

Figure DR7. Fourmile Canyon Creek.

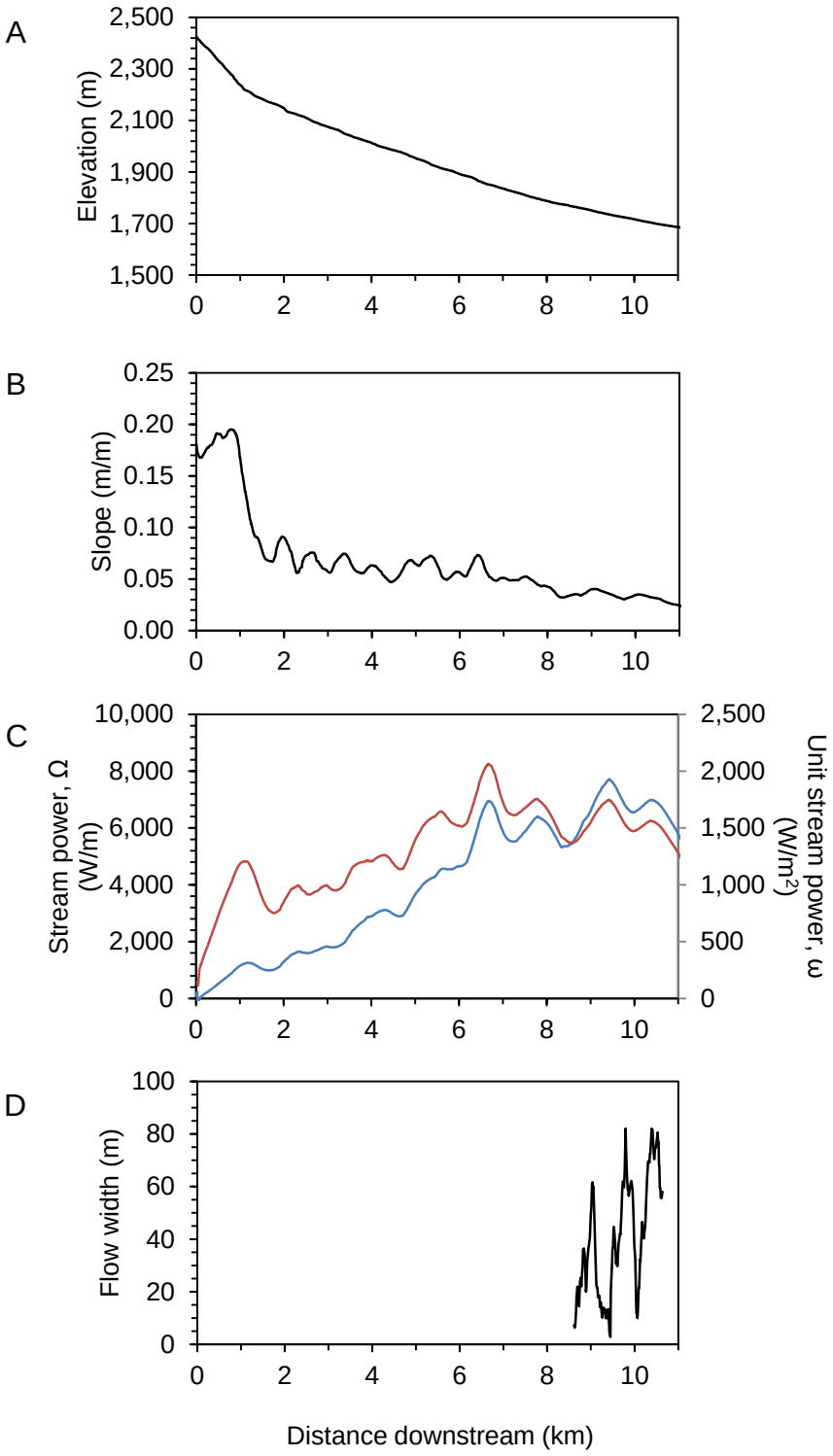

Figure DR8. Mt Sanitas channel.

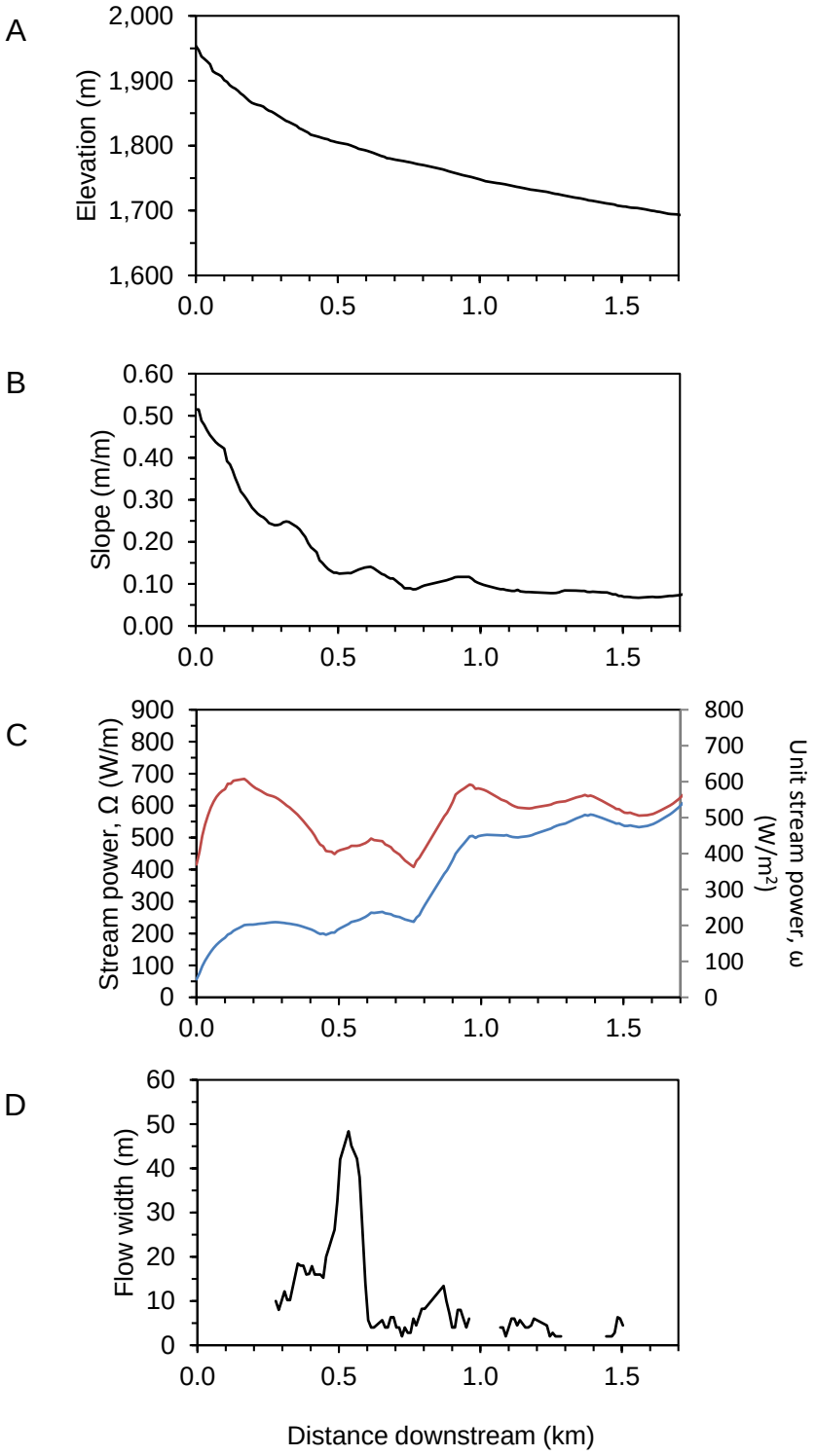

**Table DR1**

**Site characteristics**

| | Saxtons | West Br White | Fourmile Canyon | Sanitas |
|---|---|---|---|---|
| Basin area a mouth ($km^2$) | 180 | 112 | 19.4 | 0.7 |
| Channel elevation range (m) | 550 - 120 | 632 - 232 | 2419 - 1687 | 1953 - 1694 |
| Average river slope (m/m) | 0.014 | 0.025 | 0.067 | 0.15 |
| Climate | humid continental | humid continental | semi-arid | semi-arid |
| Average precipitation at mouth (cm) | 114.0 | 110.7 | 62.5 | 62.5 |
| Mean annual discharge ($m^3\ s^{-1}\ km^{-2}$) | 0.686 | 0.691 | no long term record* | no long term record* |
| Q_ref, ($m^3\ s^{-1}\ km^{-2}$) | 3.3 | 1.4 | 1.1 | 1.1 |
| Long-term regional denudation rate (mm $k.y.^{-1}$) | 3.8 - 5.6 | 3.8 - 5.6 | 30–60 | 30–60 |

* The Colorado Front Range lacks long term streamflow records where discharge primarily reflects prevailing meteorological conditions. All long term USGS gaging station have artificial diversions, storage, or other activities in or near the stream channel that affect the natural flow of the watercourse.

Table DR2a

| River | Easting* | Northing* | Distance downstream (km) | Feature | Area (m2) | Thickness estimate** (m) | Volume (m3) |
|---|---|---|---|---|---|---|---|
| West branch | 664831 | 4856128 | 1.34 | Bank failure | 30 | 0.2 | 6 |
| West branch | 664956 | 4856140 | 1.46 | Floodplain deposit | 373 | 0.2 | -- |
| West branch | 665299 | 4856190 | 1.83 | Floodplain deposit | 500 | 0.1 | -- |
| West branch | 665419 | 4856253 | 1.97 | Bank failure | 12 | 0.2 | 2 |
| West branch | 665767 | 4856269 | 2.36 | Bank failure | 25 | 0.3 | 6 |
| West branch | 665929 | 4856333 | 2.53 | Bank failure | 20 | 0.5 | 10 |
| West branch | 665947 | 4856347 | 2.57 | Bank failure | 20 | 0.5 | 10 |
| West branch | 665971 | 4856376 | 2.61 | Bank failure | 20 | 0.5 | 10 |
| West branch | 666001 | 4856414 | 2.66 | Bank failure | 20 | 0.5 | 10 |
| West branch | 666430 | 4856769 | 3.26 | Bank failure | 100 | 0.3 | 25 |
| West branch | 666492 | 4856867 | 3.40 | Floodplain deposit | 182 | 0.1 | -- |
| West branch | 666594 | 4857061 | 3.62 | Floodplain deposit | 220 | 0.1 | -- |
| West branch | 666642 | 4857112 | 3.69 | Floodplain deposit | 663 | 0.1 | -- |
| West branch | 666692 | 4857185 | 3.79 | Bank failure | 50 | 0.3 | 13 |
| West branch | 666770 | 4857272 | 3.92 | Bank failure | 15 | 0.5 | 8 |
| West branch | 667251 | 4857714 | 4.62 | Landslide | 90 | 0.5 | 45 |
| West branch | 667603 | 4857768 | 5.00 | Floodplain deposit | 1436 | 0.1 | -- |
| West branch | 667656 | 4857796 | 5.08 | Landslide | 400 | 1.0 | 400 |
| West branch | 667780 | 4857761 | 5.23 | Landslide | 250 | 1.0 | 250 |
| West branch | 668454 | 4857693 | 5.95 | Landslide | 1500 | 1.0 | 1500 |
| West branch | 668626 | 4857628 | 6.23 | Landslide | 1500 | 1.0 | 1500 |
| West branch | 668661 | 4857611 | 6.26 | Floodplain deposit | 1301 | 0.1 | -- |
| West branch | 668687 | 4857636 | 6.29 | Landslide | 60 | 1.0 | 60 |
| West branch | 668876 | 4857720 | 6.52 | Landslide | 300 | 1.0 | 300 |
| West branch | 668888 | 4857690 | 6.53 | Floodplain deposit | 2128 | 0.15 | -- |
| West branch | 668928 | 4857729 | 6.56 | Landslide | 4000 | 1.0 | 4000 |
| West branch | 669007 | 4857663 | 6.68 | Bank failure | 60 | 1.0 | 60 |
| West branch | 669473 | 4857756 | 7.19 | Floodplain deposit | 1640 | 0.2 | -- |
| West branch | 669716 | 4857797 | 7.42 | Floodplain deposit | 636 | 0.1 | -- |
| West branch | 669818 | 4857791 | 7.55 | Landslide | 1700 | 2.0 | 3400 |
| West branch | 670057 | 4858024 | 7.93 | Landslide | 3606 | 1.0 | 3606 |
| West branch | 670181 | 4858072 | 8.08 | Floodplain deposit | 1115 | 0.2 | -- |
| West branch | 670238 | 4858076 | 8.12 | Landslide | 1240 | 1.0 | 1240 |
| West branch | 670418 | 4858206 | 8.34 | Bank failure | 810 | 1.0 | 810 |
| West branch | 670611 | 4858167 | 8.56 | Floodplain deposit | 1798 | 0.2 | -- |
| West branch | 670714 | 4858184 | 8.68 | Floodplain deposit | 789 | 0.2 | -- |
| West branch | 671042 | 4858401 | 9.08 | Floodplain deposit | 7148 | 0.1 | -- |
| West branch | 671046 | 4858489 | 9.14 | Floodplain deposit | 1100 | 0.1 | -- |
| West branch | 671130 | 4858459 | 9.29 | Floodplain deposit | 10133 | 0.2 | -- |
| West branch | 671305 | 4858368 | 9.49 | Floodplain deposit | 5093 | 0.1 | -- |
| West branch | 671429 | 4858284 | 9.64 | Floodplain deposit | 5162 | 0.2 | -- |
| West branch | 671556 | 4858273 | 9.75 | Floodplain deposit | 11184 | 0.3 | -- |
| West branch | 671584 | 4858177 | 9.83 | Floodplain deposit | 5642 | 0.3 | -- |
| West branch | 671703 | 4858025 | 10.06 | Floodplain deposit | 15993 | 0.2 | -- |
| West branch | 671947 | 4857828 | 10.38 | Floodplain deposit | 4386 | 0.3 | -- |
| West branch | 672108 | 4857614 | 10.67 | Floodplain deposit | 18608 | 0.2 | -- |
| West branch | 672140 | 4857471 | 10.78 | Floodplain deposit | 4172 | 0.4 | -- |
| West branch | 672331 | 4857477 | 10.96 | Bank failure | 80 | 1.0 | 80 |
| West branch | 672333 | 4857421 | 10.99 | Floodplain deposit | 9205 | 0.4 | -- |
| West branch | 672449 | 4857474 | 11.08 | Floodplain deposit | 22169 | 0.3 | -- |
| West branch | 672581 | 4857357 | 11.24 | Floodplain deposit | 19068 | 0.4 | -- |
| West branch | 672614 | 4857478 | 11.31 | Floodplain deposit | 13283 | 0.3 | -- |

| | | | | | | | |
|---|---|---|---|---|---|---|---|
| West branch | 672751 | 4857480 | 11.47 | Floodplain deposit | 3620 | 0.4 | -- |
| West branch | 672974 | 4857614 | 11.72 | Floodplain deposit | 2499 | 0.2 | -- |
| West branch | 673256 | 4857756 | 12.03 | Landslide | 1250 | 2.0 | 2500 |
| West branch | 673298 | 4857628 | 12.14 | Floodplain deposit | 10477 | 0.2 | -- |
| West branch | 673517 | 4857541 | 12.40 | Bank failure | 350 | 2.0 | 700 |
| West branch | 673649 | 4857439 | 12.56 | Floodplain deposit | 13104 | 0.3 | -- |
| West branch | 673785 | 4857458 | 12.69 | Bank failure | 200 | 2.0 | 400 |
| West branch | 673832 | 4857482 | 12.71 | Floodplain deposit | 4011 | 0.2 | -- |
| West branch | 674039 | 4857476 | 12.97 | Floodplain deposit | 11134 | 0.2 | -- |
| West branch | 674092 | 4857430 | 13.03 | Floodplain deposit | 11544 | 0.2 | -- |
| West branch | 674246 | 4857599 | 13.26 | Floodplain deposit | 11483 | 0.2 | -- |
| West branch | 674372 | 4857497 | 13.45 | Floodplain deposit | 45186 | 0.3 | -- |
| West branch | 674518 | 4857506 | 13.58 | Landslide | 75 | 1.0 | 75 |
| West branch | 674551 | 4857423 | 13.65 | Landslide | 1750 | 2.0 | 3500 |
| West branch | 674652 | 4857544 | 13.80 | Floodplain deposit | 8516 | 0.3 | -- |
| West branch | 674931 | 4857702 | 14.12 | Landslide | 800 | 2.0 | 1600 |
| West branch | 674983 | 4857902 | 14.31 | Landslide | 600 | 2.0 | 1200 |
| West branch | 674924 | 4857892 | 14.32 | Floodplain deposit | 8136 | 0.3 | -- |
| West branch | 674985 | 4857987 | 14.49 | Floodplain deposit | 3875 | 0.3 | -- |
| West branch | 675160 | 4858011 | 14.66 | Landslide | 2000 | 2.0 | 4000 |
| West branch | 675834 | 4858622 | 15.58 | Floodplain deposit | 212593 | 0.3 | -- |

*Coordinates are in UTM zone 18, NAD 1984

** For floodplain deposits, we show an approximate measured thickness based on probing.

Given the uncertainty in some large deposits, we do not report deposition volume.

Table DR2b

| River | Easting* | Northing* | Distance downstream (km) | Feature | Area (m2) | Thickness estimate** (m) | Volume (m3) |
|---|---|---|---|---|---|---|---|
| Saxtons | 688028 | 4785162 | 3.99 | Landslide | 175 | 0.5 | 88 |
| Saxtons | 688024 | 4785161 | 4.00 | Floodplain deposit | 525 | 30.0 | -- |
| Saxtons | 688059 | 4785233 | 4.07 | Landslide | 204 | 0.5 | 102 |
| Saxtons | 688168 | 4785331 | 4.23 | Landslide | 123 | 1.5 | 184 |
| Saxtons | 688313 | 4785498 | 4.46 | Landslide | 149 | 0.5 | 74 |
| Saxtons | 688341 | 4785553 | 4.52 | Landslide | 280 | 1.5 | 420 |
| Saxtons | 688459 | 4785620 | 4.65 | Landslide | 85 | 1.0 | 85 |
| Saxtons | 688476 | 4785613 | 4.67 | Landslide | 154 | 0.8 | 116 |
| Saxtons | 688676 | 4785390 | 4.96 | Landslide | 108 | 0.5 | 54 |
| Saxtons | 688698 | 4785417 | 4.98 | Landslide | 345 | 0.5 | 173 |
| Saxtons | 688773 | 4785411 | 5.06 | Bank-failure | 658 | 1.5 | 987 |
| Saxtons | 689023 | 4785666 | 5.48 | Landslide | 171 | 1.0 | 171 |
| Saxtons | 689047 | 4785713 | 5.55 | Floodplain deposit | 464 | 15.0 | -- |
| Saxtons | 689142 | 4785814 | 5.70 | Landslide | 1440 | 1.0 | 1440 |
| Saxtons | 689178 | 4785873 | 5.77 | Landslide | 1418 | 1.0 | 1418 |
| Saxtons | 689264 | 4785999 | 5.97 | Landslide | 149 | 1.0 | 149 |
| Saxtons | 689304 | 4786027 | 6.02 | Landslide | 442 | 0.5 | 221 |
| Saxtons | 689500 | 4786026 | 6.26 | Floodplain deposit | 1140 | 50.0 | -- |
| Saxtons | 689634 | 4785977 | 6.41 | Floodplain deposit | 1639 | 20.0 | -- |
| Saxtons | 689679 | 4785948 | 6.45 | Landslide | 1400 | 0.8 | 1050 |
| Saxtons | 689731 | 4785882 | 6.53 | Bank-failure | 420 | 1.5 | 630 |
| Saxtons | 689943 | 4785829 | 6.77 | Bank-failure | 192 | 1.0 | 192 |
| Saxtons | 689943 | 4785840 | 6.78 | Floodplain deposit | 185 | 20.0 | -- |
| Saxtons | 689983 | 4785841 | 6.82 | Floodplain deposit | 217 | 15.0 | -- |
| Saxtons | 690021 | 4785845 | 6.85 | Landslide | 297 | 1.0 | 297 |
| Saxtons | 690207 | 4785830 | 7.04 | Bank-failure | 396 | 1.5 | 594 |
| Saxtons | 690305 | 4785865 | 7.15 | Landslide | 342 | 1.0 | 342 |
| Saxtons | 690659 | 4785815 | 7.56 | Floodplain deposit | 134 | 30.0 | -- |
| Saxtons | 690721 | 4785750 | 7.65 | Floodplain deposit | 995 | 5.0 | -- |
| Saxtons | 690859 | 4785563 | 7.89 | Floodplain deposit | 1597 | 50.0 | -- |
| Saxtons | 690898 | 4785512 | 7.94 | Landslide | 380 | 1.0 | 380 |
| Saxtons | 690975 | 4785455 | 8.05 | Floodplain deposit | 2038 | 5.0 | -- |
| Saxtons | 690980 | 4785396 | 8.11 | Floodplain deposit | 310 | 5.0 | -- |
| Saxtons | 690980 | 4785372 | 8.12 | Landslide | 345 | 1.0 | 345 |
| Saxtons | 691038 | 4785396 | 8.19 | Floodplain deposit | 747 | 20.0 | -- |
| Saxtons | 691266 | 4785353 | 8.45 | Floodplain deposit | 924 | 15.0 | -- |
| Saxtons | 691299 | 4785345 | 8.49 | Floodplain deposit | 1208 | 15.0 | -- |
| Saxtons | 691474 | 4785366 | 8.68 | Floodplain deposit | 1411 | 30.0 | -- |
| Saxtons | 691620 | 4785341 | 8.82 | Landslide | 180 | 1.0 | 180 |
| Saxtons | 691765 | 4785343 | 8.98 | Floodplain deposit | 6673 | 30.0 | -- |
| Saxtons | 691871 | 4785369 | 9.08 | Landslide | 662 | 2.0 | 1323 |
| Saxtons | 692088 | 4785403 | 9.33 | Floodplain deposit | 861 | 70.0 | -- |
| Saxtons | 692107 | 4785396 | 9.35 | Floodplain deposit | 13202 | 25.0 | -- |
| Saxtons | 692320 | 4785356 | 9.56 | Floodplain deposit | 3505 | 70.0 | -- |

| | | | | | | | |
|---|---|---|---|---|---|---|---|
| Saxtons | 692463 | 4785380 | 9.71 | Landslide | 165 | 1.0 | 165 |
| Saxtons | 692502 | 4785392 | 9.76 | Floodplain deposit | 915 | 70.0 | -- |
| Saxtons | 692624 | 4785433 | 9.89 | Floodplain deposit | 1514 | 94.0 | -- |
| Saxtons | 692787 | 4785461 | 10.05 | Floodplain deposit | 2235 | 25.0 | -- |
| Saxtons | 692823 | 4785472 | 10.09 | Landslide | 292 | 1.5 | 437 |
| Saxtons | 692887 | 4785522 | 10.18 | Floodplain deposit | 621 | 50.0 | -- |
| Saxtons | 693013 | 4785579 | 10.32 | Floodplain deposit | 177 | 12.0 | -- |
| Saxtons | 693111 | 4785618 | 10.42 | Floodplain deposit | 2444 | 50.0 | -- |
| Saxtons | 693221 | 4785560 | 10.57 | Floodplain deposit | 5557 | 55.0 | -- |
| Saxtons | 693335 | 4785529 | 10.69 | Floodplain deposit | 978 | 7.0 | -- |
| Saxtons | 693360 | 4785512 | 10.72 | Floodplain deposit | 1597 | 10.0 | -- |
| Saxtons | 693453 | 4785423 | 10.85 | Floodplain deposit | 1230 | 12.0 | -- |
| Saxtons | 693464 | 4785326 | 10.94 | Floodplain deposit | 783 | 30.0 | -- |
| Saxtons | 693502 | 4785204 | 11.08 | Floodplain deposit | 605 | 5.0 | -- |
| Saxtons | 693580 | 4785056 | 11.25 | Floodplain deposit | 1259 | 10.0 | -- |
| Saxtons | 693664 | 4784896 | 11.44 | Floodplain deposit | 1124 | 30.0 | -- |
| Saxtons | 693688 | 4784674 | 11.67 | Floodplain deposit | 2840 | 35.0 | -- |
| Saxtons | 693594 | 4784276 | 12.11 | Floodplain deposit | 7539 | 5.0 | -- |
| Saxtons | 693825 | 4783999 | 12.49 | Floodplain deposit | 10818 | 40.0 | -- |
| Saxtons | 693897 | 4783761 | 12.75 | Landslide | 322 | 0.5 | 161 |
| Saxtons | 693968 | 4783706 | 12.85 | Floodplain deposit | 4526 | 15.0 | -- |
| Saxtons | 694154 | 4783588 | 13.09 | Floodplain deposit | 1698 | 5.0 | -- |
| Saxtons | 694131 | 4783105 | 13.64 | Floodplain deposit | 827 | 5.0 | -- |
| Saxtons | 694256 | 4782986 | 13.82 | Floodplain deposit | 2550 | 20.0 | -- |
| Saxtons | 694342 | 4782991 | 13.91 | Floodplain deposit | 1380 | 5.0 | -- |
| Saxtons | 694402 | 4782913 | 14.01 | Floodplain deposit | 437 | 20.0 | -- |
| Saxtons | 694431 | 4782873 | 14.06 | Floodplain deposit | 520 | 25.0 | -- |
| Saxtons | 694512 | 4782809 | 14.16 | Landslide | 180 | 1.0 | 180 |
| Saxtons | 694506 | 4782811 | 14.16 | Floodplain deposit | 840 | 15.0 | -- |
| Saxtons | 695181 | 4782366 | 15.09 | Landslide | 1494 | 2.0 | 2988 |
| Saxtons | 695199 | 4782419 | 15.14 | Floodplain deposit | 3723 | 15.0 | -- |
| Saxtons | 695244 | 4782580 | 15.33 | Floodplain deposit | 3374 | 30.0 | -- |
| Saxtons | 695374 | 4782877 | 15.66 | Floodplain deposit | 2230 | -- | -- |
| Saxtons | 695637 | 4783121 | 16.06 | Floodplain deposit | 1075 | 15.0 | -- |
| Saxtons | 695795 | 4783264 | 16.28 | Floodplain deposit | 2414 | 25.0 | -- |
| Saxtons | 695869 | 4783283 | 16.36 | Floodplain deposit | 1924 | 30.0 | -- |
| Saxtons | 695906 | 4783304 | 16.40 | Bank-failure | 600 | 1.5 | 900 |
| Saxtons | 696091 | 4783366 | 16.60 | Floodplain deposit | 5251 | 10.0 | -- |
| Saxtons | 696271 | 4783336 | 16.79 | Floodplain deposit | 1085 | 5.0 | -- |
| Saxtons | 696406 | 4783315 | 16.93 | Floodplain deposit | 7994 | -- | -- |
| Saxtons | 696540 | 4783212 | 17.10 | Floodplain deposit | 9556 | -- | -- |
| Saxtons | 696589 | 4783163 | 17.17 | Floodplain deposit | 2763 | 30.0 | -- |
| Saxtons | 696827 | 4782663 | 17.74 | Floodplain deposit | 12394 | 30.0 | -- |
| Saxtons | 697055 | 4782499 | 18.03 | Floodplain deposit | 3406 | 30.0 | -- |
| Saxtons | 697056 | 4782438 | 18.08 | Landslide | 75 | 1.0 | 75 |
| Saxtons | 697018 | 4782332 | 18.21 | Floodplain deposit | 12989 | 40.0 | -- |
| Saxtons | 697018 | 4782322 | 18.22 | Floodplain deposit | 595 | 30.0 | -- |

| | | | | | | | |
|---|---|---|---|---|---|---|---|
| Saxtons | 696966 | 4782070 | 18.49 | Floodplain deposit | 652 | 10.0 | -- |
| Saxtons | 696911 | 4781918 | 18.66 | Floodplain deposit | 6115 | 35.0 | -- |
| Saxtons | 696850 | 4781472 | 19.13 | Floodplain deposit | 16611 | 35.0 | -- |
| Saxtons | 697395 | 4781119 | 20.04 | Floodplain deposit | 2931 | 10.0 | -- |
| Saxtons | 697633 | 4781165 | 20.28 | Bank-failure | 140 | 2.5 | 350 |
| Saxtons | 697735 | 4781205 | 20.40 | Floodplain deposit | 1455 | 10.0 | -- |
| Saxtons | 698038 | 4780951 | 20.81 | Floodplain deposit | 3187 | 30.0 | -- |
| Saxtons | 698376 | 4780396 | 21.49 | Floodplain deposit | 5175 | 50.0 | -- |
| Saxtons | 698436 | 4780316 | 21.59 | Floodplain deposit | 3162 | 15.0 | -- |
| Saxtons | 698451 | 4780291 | 21.62 | Floodplain deposit | 2568 | -- | -- |
| Saxtons | 698499 | 4780205 | 21.72 | Floodplain deposit | 19595 | 75.0 | -- |
| Saxtons | 698555 | 4780045 | 21.90 | Floodplain deposit | 6453 | 50.0 | -- |
| Saxtons | 698681 | 4780076 | 22.04 | Floodplain deposit | 10609 | -- | -- |
| Saxtons | 698764 | 4780057 | 22.13 | Floodplain deposit | 11391 | -- | -- |
| Saxtons | 698957 | 4780058 | 22.34 | Floodplain deposit | 23001 | 40.0 | -- |
| Saxtons | 699013 | 4780035 | 22.40 | Floodplain deposit | 4179 | -- | -- |
| Saxtons | 699186 | 4779996 | 22.59 | Floodplain deposit | 16541 | 5.0 | -- |
| Saxtons | 699397 | 4779838 | 22.88 | Floodplain deposit | 22764 | 40.0 | -- |
| Saxtons | 699693 | 4779787 | 23.22 | Floodplain deposit | 17559 | -- | -- |
| Saxtons | 699829 | 4779757 | 23.37 | Floodplain deposit | 9263 | 40.0 | -- |
| Saxtons | 699924 | 4779546 | 23.60 | Floodplain deposit | 11248 | 40.0 | -- |
| Saxtons | 700125 | 4779392 | 23.87 | Bank-failure | 440 | 1.0 | 440 |
| Saxtons | 700259 | 4779247 | 24.09 | Landslide | 100 | 0.5 | 50 |
| Saxtons | 700331 | 4779234 | 24.16 | Bank-failure | 1080 | 2.0 | 2160 |
| Saxtons | 700655 | 4779194 | 24.52 | Floodplain deposit | 2530 | 5.0 | -- |
| Saxtons | 700716 | 4779133 | 24.60 | Bank-failure | 384 | 1.0 | 384 |
| Saxtons | 701086 | 4778896 | 25.05 | Bank-failure | 400 | 1.5 | 600 |
| Saxtons | 701161 | 4778879 | 25.14 | Floodplain deposit | 2039 | 10.0 | -- |
| Saxtons | 701487 | 4778812 | 25.47 | Floodplain deposit | 14400 | 20.0 | -- |
| Saxtons | 701539 | 4778782 | 25.53 | Floodplain deposit | 15517 | 25.0 | -- |
| Saxtons | 701666 | 4778753 | 25.67 | Bank-failure | 75 | 0.5 | 38 |
| Saxtons | 701832 | 4778716 | 25.85 | Floodplain deposit | 8011 | 15.0 | -- |
| Saxtons | 701927 | 4778669 | 25.96 | Floodplain deposit | 8403 | -- | -- |
| Saxtons | 702100 | 4778727 | 26.17 | Floodplain deposit | 24067 | 40.0 | -- |
| Saxtons | 702079 | 4778920 | 26.39 | Floodplain deposit | 23586 | -- | -- |
| Saxtons | 702131 | 4779099 | 26.61 | Floodplain deposit | 9964 | 30.0 | -- |
| Saxtons | 702811 | 4779003 | 27.36 | Landslide | 1320 | 1.0 | 1320 |
| Saxtons | 702811 | 4779003 | 27.36 | Landslide | 780 | 1.5 | 1170 |
| Saxtons | 703062 | 4779231 | 27.76 | Floodplain deposit | 1580 | 40.0 | -- |
| Saxtons | 703205 | 4779446 | 28.03 | Floodplain deposit | 3320 | -- | -- |
| Saxtons | 703484 | 4779539 | 28.33 | Floodplain deposit | 3819 | 20.0 | -- |
| Saxtons | 703770 | 4779617 | 28.63 | Floodplain deposit | 2403 | 15.0 | -- |
| Saxtons | 704083 | 4779407 | 29.02 | Floodplain deposit | 1289 | 50.0 | -- |

*Coordinates are in UTM zone 18, NAD 1984

** For floodplain deposits, we show the maximum measured thickness based on probing.

Given the uncertainty in some large deposits, we do not report deposition volume.

Table DR2c

| River | Easting* | Northing* | Distance downstream (m) | Feature | Volume (m3) | Erosion or deposition |
|---|---|---|---|---|---|---|
| Sanitas | 474114 | 4431471 | 0 | debris flow | 120 | Erosion |
| Sanitas | 474125 | 4431482 | 10 | bank widening, channel incision | 56 | Erosion |
| Sanitas | 474161 | 4431481 | 50 | debris flow | 192 | Erosion |
| Sanitas | 474175 | 4431491 | 60 | bank widening, channel incision | 90 | Erosion |
| Sanitas | 474183 | 4431494 | 70 | bank widening, channel incision | 114 | Erosion |
| Sanitas | 474225 | 4431488 | 120 | bank widening, channel incision | 160 | Erosion |
| Sanitas | 474251 | 4431487 | 138 | bank widening, channel incision | 280 | Erosion |
| Sanitas | 474287 | 4431483 | 178 | bank widening, channel incision | 240 | Erosion |
| Sanitas | 474315 | 4431481 | 208 | bank widening, channel incision | 270 | Erosion |
| Sanitas | 474367 | 4431470 | 267 | bank widening, channel incision | 200 | Erosion |
| Sanitas | 474448 | 4431448 | 355 | bank widening, channel incision | 50 | Erosion |
| Sanitas | 474448 | 4431448 | 355 | near channel deposition | 225 | Deposition |
| Sanitas | 474448 | 4431448 | 355 | near channel deposition | 400 | Deposition |
| Sanitas | 474899 | 4430077 | 415 | bank widening, channel incision | 100 | Erosion |
| Sanitas | 474899 | 4430077 | 415 | near channel deposition | 675 | Deposition |
| Sanitas | 474899 | 4430077 | 484 | near channel deposition | 65 | Deposition |
| Sanitas | 474899 | 4430077 | 613 | bank widening, channel incision | 8 | Erosion |
| Sanitas | 474899 | 4430077 | 643 | near channel deposition | 24 | Deposition |
| Sanitas | 474899 | 4430077 | 663 | bank widening, channel incision | 27 | Erosion |
| Sanitas | 474899 | 4430077 | 723 | bank widening, channel incision | 23 | Erosion |
| Sanitas | 474899 | 4430077 | 783 | bank widening, channel incision | 45 | Erosion |
| Sanitas | 474899 | 4430077 | 842 | bank widening, channel incision | 10 | Erosion |
| Sanitas | 474899 | 4430077 | 893 | bank widening, channel incision | 75 | Erosion |
| Sanitas | 474669 | 4431044 | 933 | bank widening, channel incision | 100 | Erosion |
| Sanitas | 474654 | 4430969 | 993 | bank widening, channel incision | 98 | Erosion |
| Sanitas | 474655 | 4430943 | 1023 | bank widening, channel incision | 35 | Erosion |
| Sanitas | 474899 | 4430077 | 1052 | near channel deposition | 15 | Deposition |
| Sanitas | 474899 | 4430077 | 1063 | bank widening, channel incision | 20 | Erosion |
| Sanitas | 474899 | 4430077 | 1073 | bank widening, channel incision | 100 | Erosion |
| Sanitas | 474899 | 4430077 | 1073 | near channel deposition | 88 | Deposition |
| Sanitas | 474899 | 4430077 | 1143 | near channel deposition | 36 | Deposition |
| Sanitas | 474899 | 4430077 | 1162 | bank widening, channel incision | 38 | Erosion |
| Sanitas | 474899 | 4430077 | 1241 | bank widening, channel incision | 38 | Erosion |
| Sanitas | 474660 | 4430721 | 1251 | bank widening, channel incision | 25 | Erosion |
| Sanitas | 474899 | 4430077 | 1311 | near channel deposition | 3 | Deposition |
| Sanitas | 474899 | 4430077 | 1431 | near channel deposition | 180 | Deposition |
| Sanitas | 474899 | 4430077 | 1460 | near channel deposition | 23 | Deposition |
| Sanitas | 474899 | 4430077 | 1470 | bank widening, channel incision | 150 | Erosion |
| Sanitas | 474899 | 4430077 | 1490 | bank widening, channel incision | 31 | Erosion |
| Sanitas | 474899 | 4430077 | 1510 | near channel deposition | 70 | Deposition |
| Sanitas | 474899 | 4430077 | 1540 | near channel deposition | 225 | Deposition |
| Sanitas | 474899 | 4430077 | 1550 | bank widening, channel incision | 2 | Erosion |
| Sanitas | 474899 | 4430077 | 1590 | near channel deposition | 20 | Deposition |
| Sanitas | 474899 | 4430077 | 1609 | near channel deposition | 0 | Deposition |
| Sanitas | 474899 | 4430077 | 1750 | bank widening, channel incision | 3 | Erosion |
| Sanitas | 474899 | 4430077 | 1759 | near channel deposition | 2 | Deposition |
| Sanitas | 474899 | 4430077 | 1769 | near channel deposition | 1 | Deposition |

*Coordinates are in UTM zone 13, NAD 1984

Table DR2d

| River | Easting* | Northing* | Distance downstream (km) | Feature | Volume (m3) | Erosion or deposition |
|---|---|---|---|---|---|---|
| Fourmile | 472090 | 4434058 | 6.19 | bank erosion | 10 | erosion |
| Fourmile | 472118 | 4434054 | 6.22 | bank erosion | 50 | erosion |
| Fourmile | 472127 | 4434056 | 6.23 | floodplain deposit | 25 | deposition |
| Fourmile | 472163 | 4434074 | 6.27 | bank erosion | 240 | erosion |
| Fourmile | 472172 | 4434079 | 6.28 | bank erosion | 30 | erosion |
| Fourmile | 472181 | 4434083 | 6.29 | landslide | 230 | erosion |
| Fourmile | 472199 | 4434092 | 6.31 | bank erosion | 54 | erosion |
| Fourmile | 472226 | 4434105 | 6.34 | floodplain stripping | 66 | erosion |
| Fourmile | 472285 | 4434115 | 6.40 | floodplain deposit | 37 | deposition |
| Fourmile | 472310 | 4434126 | 6.42 | bank erosion | 120 | erosion |
| Fourmile | 472320 | 4434126 | 6.43 | bank erosion | 3 | erosion |
| Fourmile | 472360 | 4434125 | 6.47 | floodplain deposit | 115 | deposition |
| Fourmile | 472370 | 4434125 | 6.48 | bank erosion | 1 | erosion |
| Fourmile | 472370 | 4434125 | 6.48 | floodplain deposit | 200 | deposition |
| Fourmile | 472370 | 4434125 | 6.48 | landslide | 1000 | erosion |
| Fourmile | 472390 | 4434125 | 6.50 | bank erosion | 8 | erosion |
| Fourmile | 472400 | 4434125 | 6.51 | gully erosion | 9000 | erosion |
| Fourmile | 472418 | 4434129 | 6.53 | bank erosion | 40 | erosion |
| Fourmile | 472424 | 4434177 | 6.58 | bank erosion and avulsion | 4 | erosion |
| Fourmile | 472406 | 4434252 | 6.67 | floodplain deposit | 4 | deposition |
| Fourmile | 472424 | 4434259 | 6.69 | landslide | 225 | erosion |
| Fourmile | 472434 | 4434259 | 6.70 | bank erosion | 6 | erosion |
| Fourmile | 472434 | 4434259 | 6.70 | floodplain deposit | 15 | deposition |
| Fourmile | 472444 | 4434259 | 6.71 | bank erosion and avulsion | 55 | erosion |
| Fourmile | 472464 | 4434259 | 6.73 | bank erosion | 8 | erosion |
| Fourmile | 472494 | 4434259 | 6.76 | floodplain deposit | 6 | deposition |
| Fourmile | 472514 | 4434258 | 6.78 | bank erosion | 17 | erosion |
| Fourmile | 472534 | 4434258 | 6.80 | landslide | 3200 | erosion |
| Fourmile | 472584 | 4434258 | 6.85 | floodplain deposit | 3 | deposition |
| Fourmile | 472594 | 4434258 | 6.86 | bank erosion | 10 | erosion |
| Fourmile | 472609 | 4434269 | 6.88 | floodplain deposit | 113 | deposition |
| Fourmile | 472639 | 4434296 | 6.92 | bank erosion | 200 | erosion |
| Fourmile | 472639 | 4434296 | 6.92 | floodplain deposit | 420 | deposition |
| Fourmile | 472690 | 4434343 | 6.99 | floodplain deposit | 2 | deposition |
| Fourmile | 472690 | 4434343 | 6.99 | landslide | 2000 | erosion |
| Fourmile | 472725 | 4434364 | 7.03 | floodplain deposit | 180 | deposition |
| Fourmile | 472785 | 4434399 | 7.10 | gully erosion | 900 | erosion |
| Fourmile | 472889 | 4434475 | 7.23 | bank erosion | 240 | erosion |
| Fourmile | 472939 | 4434546 | 7.32 | floodplain deposit | 20 | deposition |
| Fourmile | 472947 | 4434552 | 7.33 | floodplain deposit | 40 | deposition |
| Fourmile | 472963 | 4434564 | 7.35 | bank erosion | 367 | erosion |
| Fourmile | 473073 | 4434554 | 7.47 | landslide | 654 | erosion |
| Fourmile | 473099 | 4434564 | 7.50 | landslide | 1523 | erosion |
| Fourmile | 473290 | 4434780 | 7.82 | bank erosion | 92 | erosion |
| Fourmile | 473334 | 4434793 | 7.87 | unclassified erosion | 222 | erosion |
| Fourmile | 473465 | 4434876 | 8.03 | floodplain deposit | 150 | deposition |
| Fourmile | 473544 | 4434887 | 8.11 | unclassified erosion | 788 | erosion |
| Fourmile | 473594 | 4434891 | 8.16 | unclassified erosion | 819 | erosion |
| Fourmile | 473657 | 4434937 | 8.24 | unclassified erosion | 277 | erosion |
| Fourmile | 473710 | 4434983 | 8.31 | unclassified erosion | 457 | erosion |
| Fourmile | 473754 | 4434996 | 8.36 | unclassified erosion | 179 | erosion |
| Fourmile | 473824 | 4434957 | 8.44 | unclassified erosion | 620 | erosion |
| Fourmile | 473876 | 4434952 | 8.50 | unclassified erosion | 235 | erosion |

| | | | | | | |
|---|---|---|---|---|---|---|
| Fourmile | 473886 | 4434952 | 8.51 | unclassified erosion | 120 | erosion |
| Fourmile | 473896 | 4434952 | 8.52 | unclassified erosion | 75 | erosion |
| Fourmile | 474000 | 4434983 | 8.63 | floodplain deposit | 120 | deposition |
| Fourmile | 474047 | 4434990 | 8.68 | floodplain deposit | 400 | deposition |
| Fourmile | 474107 | 4434984 | 8.74 | unclassified erosion | 496 | erosion |
| Fourmile | 474197 | 4434993 | 8.84 | floodplain deposit | 120 | deposition |
| Fourmile | 474227 | 4434996 | 8.87 | floodplain deposit | 60 | deposition |
| Fourmile | 474237 | 4434997 | 8.88 | floodplain deposit | 14 | deposition |
| Fourmile | 474277 | 4435002 | 8.92 | floodplain deposit | 83 | deposition |
| Fourmile | 474380 | 4434934 | 9.04 | floodplain deposit | 281 | deposition |
| Fourmile | 474390 | 4434931 | 9.06 | unclassified erosion | 500 | erosion |
| Fourmile | 474427 | 4434898 | 9.11 | unclassified erosion | 120 | erosion |
| Fourmile | 474462 | 4434879 | 9.15 | unclassified erosion | 500 | erosion |
| Fourmile | 474527 | 4434856 | 9.22 | unclassified erosion | 2040 | erosion |
| Fourmile | 474597 | 4434849 | 9.29 | unclassified erosion | 100 | erosion |
| Fourmile | 474597 | 4434849 | 9.29 | floodplain deposit | 300 | deposition |
| Fourmile | 474597 | 4434849 | 9.29 | unclassified erosion | 600 | erosion |
| Fourmile | 474636 | 4434845 | 9.33 | floodplain deposit | 720 | deposition |
| Fourmile | 474636 | 4434845 | 9.33 | unclassified erosion | 2400 | erosion |
| Fourmile | 474716 | 4434837 | 9.41 | unclassified erosion | 800 | erosion |
| Fourmile | 474771 | 4434826 | 9.47 | unclassified erosion | 700 | erosion |
| Fourmile | 474781 | 4434826 | 9.48 | unclassified erosion | 675 | erosion |
| Fourmile | 474821 | 4434826 | 9.52 | unclassified erosion | 2304 | erosion |
| Fourmile | 474859 | 4434834 | 9.55 | floodplain deposit | 360 | deposition |
| Fourmile | 474859 | 4434834 | 9.56 | unclassified erosion | 840 | erosion |
| Fourmile | 474886 | 4434847 | 9.58 | floodplain deposit | 15221 | deposition |
| Fourmile | 474904 | 4434856 | 9.61 | bank erosion | 682 | erosion |
| Fourmile | 474922 | 4434865 | 9.63 | floodplain deposit | 202 | deposition |
| Fourmile | 475035 | 4434864 | 9.75 | floodplain deposit | 5585 | deposition |
| Fourmile | 475110 | 4434785 | 9.86 | floodplain deposit | 265 | deposition |
| Fourmile | 475116 | 4434777 | 9.87 | floodplain deposit | 2588 | deposition |
| Fourmile | 475178 | 4434690 | 9.97 | bank erosion | 102 | erosion |
| Fourmile | 475263 | 4434670 | 10.06 | unclassified erosion | 89 | erosion |
| Fourmile | 475368 | 4434571 | 10.21 | floodplain deposit | 1805 | deposition |
| Fourmile | 475371 | 4434561 | 10.22 | bank erosion | 478 | erosion |
| Fourmile | 475417 | 4434432 | 10.37 | floodplain deposit | 48 | deposition |
| Fourmile | 475431 | 4434418 | 10.39 | floodplain deposit | 209 | deposition |
| Fourmile | 475452 | 4434396 | 10.42 | bank erosion | 454 | erosion |
| Fourmile | 475517 | 4434310 | 10.53 | bank erosion | 419 | erosion |
| Fourmile | 475574 | 4434273 | 10.60 | floodplain deposit | 86 | deposition |
| Fourmile | 475590 | 4434261 | 10.62 | floodplain deposit | 2642 | deposition |

*Coordinates are in UTM zone 13, NAD 1984

Table DR3. Relationship between flow widening, narrowing, erosion, and deposiiton in locations where flow areas not obscured by vegetation in immediate post flood aerial imagery

| A. Flood flow width widens | | | | |
|---|---|---|---|---|
| | # of locations | deposition | erosion | no response |
| sanitas | 3 | 1 | 0 | 2 |
| 4 mile | 4 | 2 | 1 | 1 |
| west branch | 7 | 5 | 1 | 1 |
| saxtons | | insufficient imagery | | |
| sum | 14 | 8 | 2 | 4 |
| percentage | | 57% | 14% | 29% |

| B. Flood flow width narrows | | | | |
|---|---|---|---|---|
| | # of locations | deposition | erosion | no response |
| sanitas | 2 | 0 | 1 | 1 |
| 4 mile | 4 | 3 | 1 | 0 |
| west branch | 5 | 2 | 2 | 1 |
| saxtons | | insufficient imagery | | |
| sum | 11 | 5 | 4 | 2 |
| percentage | | 36% | 29% | 14% |